Article

Characterization of the Cation and Temperature Dependence of DNA Quadruplex Hydrogen Bond Properties Using High-Resolution NMR

Andrew J. Dingley, Robert D. Peterson, Stephan Grzesiek, and Juli Feigon

J. Am. Chem. Soc., **2005**, 127 (41), 14466-14472• DOI: 10.1021/ja0540369 • Publication Date (Web): 27 September 2005

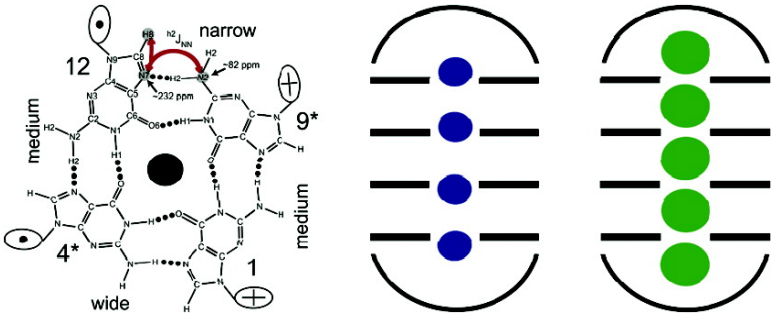

More About This Article

Additional resources and features associated with this article are available within the HTML version:

- Supporting Information
- Links to the 7 articles that cite this article, as of the time of this article download
- Access to high resolution figures
- Links to articles and content related to this article
- Copyright permission to reproduce figures and/or text from this article

View the Full Text HTML

J|A|C|S
ARTICLES
Published on Web 09/27/2005

Characterization of the Cation and Temperature Dependence of DNA Quadruplex Hydrogen Bond Properties Using High-Resolution NMR

Andrew J. Dingley,*,† Robert D. Peterson,‡ Stephan Grzesiek,*,§ and Juli Feigon*,‡

Contribution from the Department of Biochemistry and Molecular Biology, University College London, Gower Street, London WC1E 6BT, U.K., Department of Chemistry and Biochemistry and Molecular Biology Institute, University of California, Los Angeles, California 90095-1569, and Department of Structural Biology, Biozentrum, University of Basel, CH-4056 Basel, Switzerland

Received June 17, 2005; E-mail: dingley@biochem.ucl.ac.uk; stephan.grzesiek@unibas.ch; feigon@mbi.ucla.edu

Abstract: Variations in the hydrogen bond network of the Oxy-1.5 DNA guanine quadruplex have been monitored by *trans*-H-bond scalar couplings, $^{h2}J_{N2N7}$, for Na^+-, K^+-, and NH_4^+-bound forms over a temperature range from 5 to 55 °C. The variations in $^{h2}J_{N2N7}$ couplings exhibit an overall trend of $Na^+ > K^+ > NH_4^+$ and correlate with the different cation positions and N2−H2···N7 H-bond lengths in the respective structures. A global weakening of the $^{h2}J_{N2N7}$ couplings with increasing temperature for the three DNA quadruplex species is accompanied by a global increase of the acceptor ^{15}N7 chemical shifts. Above 35 °C, spectral heterogeneity indicates thermal denaturation for the Na^+-bound form, whereas spectral homogeneity persists up to 55 °C for the K^+- and NH_4^+-coordinated forms. The average relative change of the $^{h2}J_{N2N7}$ couplings amounts to $\sim 0.8 \times 10^{-3}$/K and is thus considerably smaller than respective values reported for nucleic acid duplexes. The significantly higher thermal stability of H-bond geometries in the DNA quadruplexes can be rationalized by their cation coordination of the G-quartets and the extensive H-bond network between the four strands. A detailed analysis of individual $^{h2}J_{N2N7}$ couplings reveals that the 5′ strand end, comprising base pairs G1−G9* and G4*−G1, is the most thermolabile region of the DNA quadruplex in all three cation-bound forms.

Introduction

Hydrogen bond networks are of central importance in the folding and stability of macromolecules. Recent developments in NMR have made it possible to detect the presence of hydrogen bonds via measurement of electron-mediated scalar couplings between magnetic nuclei on both sides of a hydrogen bond (H-bond) in a wide range of biomacromolecules[1−12] and smaller chemical compounds.[13−15] Such H-bond scalar couplings (HBCs) can be used to directly identify individual H-bond partners within biological macromolecules by simple COSY experiments. In particular, for nucleic acids, the substantial $^{h2}J_{NN}$ couplings (i.e., 5−11 Hz)[1,2,16] in the abundant N−H···N H-bond moiety provide valuable structural information.[1,11,16] Experimental and quantum chemical studies have shown that the size of the H-bond scalar couplings depends strongly on the H-bond geometry, in particular, the H-bond distance, for which an approximately exponential decay is observed.[5,17,18] Consequently, variations in the HBCs can be used as an indicator of changes in H-bond geometry in various situations, such as ligand binding,[19] temperature and pressure variations,[20−23] peptide folding,[24] and redox reactions.[25]

In the present study, we have applied a similar approach to characterize the ion-dependence and temperature stability of the H-bond network in the guanine quartets (G-quartets)[26] of a DNA

† University College London.
‡ University of California.
§ University of Basel.

(1) Dingley, A. J.; Grzesiek, S. *J. Am. Chem. Soc.* **1998**, *120*, 8293−8297.
(2) Pervushin, K.; Ono, A.; Fernandez, C.; Szyperski, T.; Kainosho, M.; Wuthrich, K. *Proc. Natl. Acad. Sci. U.S.A.* **1998**, *95*, 14147−14151.
(3) Cordier, F.; Grzesiek, S. *J. Am. Chem. Soc.* **1999**, *121*, 1601−1602.
(4) Cordier, F.; Rogowski, M.; Grzesiek, S.; Bax, A. *J. Magn. Reson.* **1999**, *140*, 510−512.
(5) Cornilescu, G.; Ramirez, B. E.; Frank, M. K.; Clore, G. M.; Gronenborn, A. M.; Bax, A. *J. Am. Chem. Soc.* **1999**, *121*, 6275−6279.
(6) Cornilescu, G.; Hu, J.-S.; Bax, A. *J. Am. Chem. Soc.* **1999**, *121*, 2949−2950.
(7) Majumdar, A.; Kettani, A.; Skripkin, E.; Patel, D. J. *J. Biomol. NMR* **1999**, *15*, 207−211.
(8) Löhr, F.; Mayhew, S. G.; Rüterjans, H. *J. Am. Chem. Soc.* **2000**, *122*, 9289−9295.
(9) Mishima, M.; Hatanaka, M.; Yokoyama, S.; Ikegami, T.; Wälchli, M.; Ito, Y.; Shirakawa, M. *J. Am. Chem. Soc.* **2000**, *122*, 5883−5884.
(10) Dingley, A. J.; Cordier, F.; Grzesiek, S. *Concepts Magn. Reson.* **2001**, *13*, 103−127.
(11) Grzesiek, S.; Cordier, F.; Dingley, A. J. *Methods Enzymol.* **2001**, *338*, 111−133.
(12) Grzesiek, S.; Cordier, F.; Jaravine, V.; Barfield, M. *Prog. NMR Spectrosc.* **2004**, *45*, 275−300.
(13) Kwon, O.; Danishefsky, S. *J. Am. Chem. Soc.* **1998**, *120*, 1588−1599.
(14) Shenderovich, I. G.; Smirnov, S. N.; Denisov, G. S.; Gindin, V. A.; Golubev, N. S.; Dunger, A.; Reibke, R.; Kirpekar, S.; Malkina, O. L.; Limbach, H.-H. *Ber. Bunsen-Ges. Phys. Chem.* **1998**, *102*, 422−428.
(15) Golubev, N. S.; Shenderovich, I. G.; Smirnov, S. N.; Denisov, G. S.; Limbach, H.-H. *Chem.−Eur. J.* **1999**, *5*, 492−497.
(16) Dingley, A. J.; Masse, J. E.; Peterson, R. D.; Barfield, M.; Feigon, J.; Grzesiek, S. *J. Am. Chem. Soc.* **1999**, *121*, 6019−6027.
(17) Scheurer, C.; Brüschweiler, R. *J. Am. Chem. Soc.* **1999**, *121*, 8661−8662.
(18) Barfield, M.; Dingley, A. J.; Feigon, J.; Grzesiek, S. *J. Am. Chem. Soc.* **2001**, *123*, 4014−4022.
(19) Cordier, F.; Wang, C.; Grzesiek, S.; Nicholson, L. K. *J. Mol. Biol.* **2000**, *304*, 497−505.
(20) Kojima, C.; Ono, A.; Kainosho, M. *J. Biomol. NMR* **2000**, *18*, 269−277.

10.1021/ja0540369 CCC: $30.25

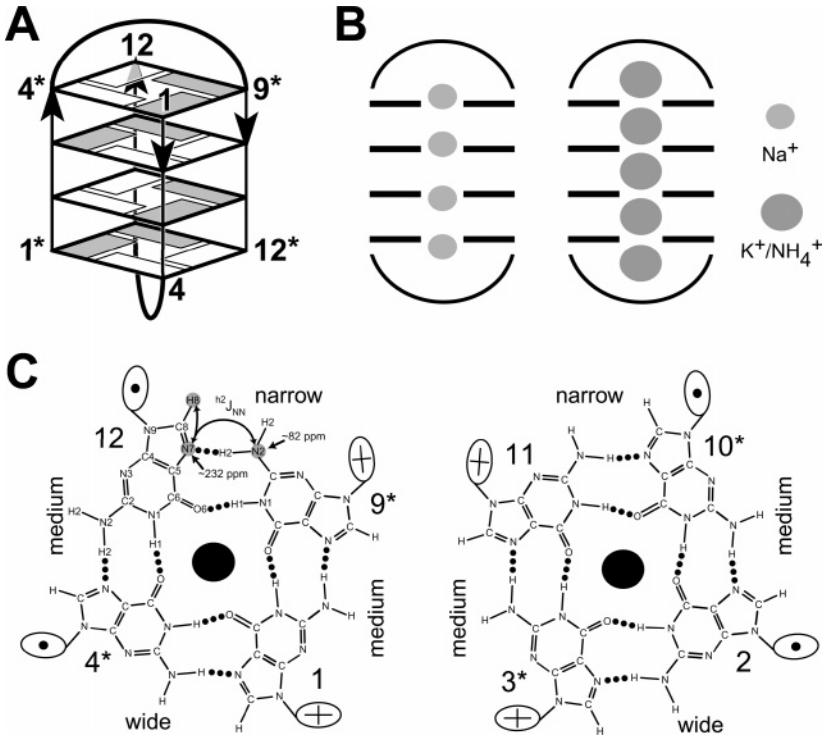

Figure 1. (A) Schematic structure of the Oxy-1.5 DNA quadruplex formed by two d($G_4T_4G_4$) strands. The arrows indicate the strand direction, and *syn* and *anti* guanine nucleotides are shaded and white rectangles, respectively. The thymines form the diagonal loops that span the end quartets. Residue numbers marked with an asterisk represent the second strand. (B) Position of monovalent cations in the DNA quadruplexes. The smaller Na^+ ion coordinates within the planes of the G-quartets, whereas the larger K^+ and NH_4^+ ions are sandwiched symmetrically between two planes of G-quartets. Coordination in all DNA quadruplex species involves the O6 of the guanine base, which points toward the central cavity occupied by the monovalent cations. In the crystal structure of the K^+-bound Oxy-1.5 DNA quadruplex,[36] cations are observed to also coordinate in the thymine loops. (C) Chemical structure of the inner and outer G-quartets. Double-headed arrows represent the magnetization pathway of the quantitative J_{NN} constant-time spin−echo difference experiment used for the observation of $^{h2}J_{N2N7}$ *trans*-H-bond scalar couplings. The black filled circle in the center of the G-quartets represents the position of the cation.

quadruplex, which is formed by a C_2-symmetric dimer of the oligonucleotide d($G_4T_4G_4$) (Oxy-1.5) (Figure 1). The Oxy-1.5 quadruplex contains the repeat sequence d(T_4G_4) found in the telomeres of the protozoan *Oxytricha nova*. Quadruplexes that form from such telomere repeats and in other regions of the genome may play important biological roles[27−31] and require monovalent or small divalent cations for the preservation of structural integrity. Structures of the sodium[32,33] and potassium[34] bound forms of Oxy-1.5 quadruplex have been solved by solution NMR and agree with more recent crystal structures.[35,36] Both cation-bound forms have the same folding topology, where the 16-guanine bases of the two monomers build a central core of four stacked hydrogen-bonded guanine quartets, and the thymines of each monomer form ordered loops connecting diagonally opposed corners of the bottom and top G-quartets. NMR studies have indicated that the ammonium ion-bound form of the Oxy-1.5 quadruplex has a similar structure to the potassium form.[34]

The monovalent cation positions as well as details of the loop conformations differ between the sodium and potassium quadruplex structures (Figure 1B). In the crystal structure of the K^+ form of Oxy-1.5 (PDB entry 1JPQ) solved to 1.5 Å resolution five equally spaced ions are observed:[36] three potassium ions are embedded between the planes of the quartets, and two are coordinated within each thymine loop. The binding sites for the centrally placed K^+ ions agree with NMR results on the NH_4^+ form.[34] However, no NH_4^+ binding sites could be detected by NMR in the thymine loops, indicating either that NH_4^+ ions do not coordinate in the loops in solution or that the relative affinity is lower in the loops than between the quartets. In the crystal structure of the Na^+ form of Oxy-1.5 solved to 1.9 Å resolution (PDB entry 1JB7) four ions are observed:[35] two central Na^+ ions are nearly coplanar with the central guanosine quartets, and the outer two Na^+ ions are positioned just above the planes of the outer quartets and toward the thymine loops. The inner Na^+ ions are coordinated by the inner quartet guanosine carbonyl oxygens, whereas[34] the two outer Na^+ ions are in addition coordinated by the thymine O2 atoms, thereby providing conformational stability to the thymine loops.

(21) Cordier, F.; Grzesiek, S. *J. Mol. Biol.* **2002**, *317*, 739−752.
(22) Li, H.; Yamada, H.; Akasaka, K.; Gronenborn, A. M. *J. Biomol. NMR* **2000**, *18*, 207−216.
(23) Bytchenkoff, B.; Chiarparin, E.; Früh, S.; Rüdisser, S.; Bodenhausen, G. *Magn. Reson. Chem.* **2002**, *40*, 377−379.
(24) Jaravine, V. A.; Alexandrescu, A. T.; Grzesiek, S. *Protein Sci.* **2001**, *10*, 943−950.
(25) Löhr, F.; Yalloway, G. N.; Mayhew, S. G.; Rüterjans, H. *Chembiochem.* **2004**, *5*, 1523−1534.
(26) Guschlbauer, W.; Chantot, J. F.; Thiele, D. *J. Biomol. Struct. Dyn.* **1990**, *8*, 491−511.
(27) McEachern, M. J.; Krauskopf, A.; Blackburn, E. H. *Annu. Rev. Genet.* **2000**, *34*, 331−358.
(28) Blackburn, E. H. *Cell* **2001**, *106*, 661−673.
(29) Davis, J. T. *Angew. Chem., Int. Ed.* **2004**, *43*, 668−698.
(30) Arthanari, H.; Bolton, P. H. *Chem. Biol.* **2001**, *8*, 221−230.
(31) Ding, H.; Schertzer, M.; Wu, X.; Gertsenstein, M.; Selig, S.; Kammori, M.; Pourvali, R.; Poon, S.; Vulto, I.; Chavez, E.; Tam, P. P.; Nagy, A.; Lansdorp, P. M. *Cell* **2004**, *117*, 873−886.
(32) Smith, F. W.; Feigon, J. *Nature* **1992**, *356*, 164−168.
(33) Schultze, P.; Smith, F. W.; Feigon, J. *Structure* **1994**, *2*, 221−233.
(34) Schultze, P.; Hud, N. V.; Smith, F. W.; Feigon, J. *Nucleic Acids Res.* **1999**, *27*, 3018−3028.
(35) Horvath, M. P.; Schultz, S. C. *J. Mol. Biol.* **2001**, *310*, 367−377.
(36) Haider, S.; Parkinson, G. N.; Neidle, S. *J. Mol. Biol.* **2002**, *320*, 189−200.

The observed differences in the coordination positions of the K^+ (and NH_4^+) and Na^+ ions are attributed to the different ionic radii of the ions.[37,38] The smaller Na^+ ion is capable of residing within the plane of a G-quartet, whereas the larger K^+ and NH_4^+ ions coordinate between two G-quartets. Further, the Na^+ ion is less constrained by steric clashes than K^+ and NH_4^+ and can occupy a range of positions that reduce electrostatic repulsion between the adjacent ions. Thermodynamic studies examining ion selectivity of the DNA quadruplex have shown that the K^+ ion rather than the Na^+ ion is preferred.[39] Apparently, the preference of K^+ over Na^+ is primarily due to the greater cost of Na^+ dehydration with respect to K^+, whereas the intrinsic free energy of Na^+ binding by G-quartets is more favorable than that of K^+.[39,40] NMR experiments have shown that NH_4^+ ions move between the G-quartet layers and out into solution, thus indicating that all ions probably shuttle to and from the ion binding sites.[41]

Although NMR NOE cross-peak patterns are very similar for the Na^+ and K^+ forms of the Oxy-1.5 quadruplex,[34] large chemical shift differences between the two forms for many of the resonances clearly indicate subtle differences in the arrangement of the guanine bases and the spacing between the G-quartets. Each of the four G-quartets contains four N1−H1···O6═C6 and four N2−H2···N7 H-bonds (Figure 1). We have shown previously that the N1−H1···O6═C6 H-bonds can be detected by the small (∼0.2 Hz) $^{h3}J_{N1C6'}$ couplings, whereas the N2−H2···N7 H-bonds are detectable by the larger (∼7 Hz) $^{h2}J_{N2N7}$ couplings.[42]

In an effort to understand the influence of the monovalent cations on the Oxy-1.5 quadruplex structure and stability, we have carried out a systematic quantitative analysis of the $^{h2}J_{N2N7}$ couplings in the Na^+, K^+, and NH_4^+ forms of the Oxy-1.5 quadruplex over a temperature range of 5−55 °C. The observed variations in $^{h2}J_{N2N7}$ couplings between DNA quadruplex species reflect genuine structural differences in H-bond geometry. In particular, the generally larger sizes of the $^{h2}J_{N2N7}$ couplings for the Na^+-bound Oxy-1.5 quadruplex are attributed to the different coordination position of the Na^+ versus K^+/NH_4^+ ions in the structures. The results show an overall weakening of the $^{h2}J_{N2N7}$ couplings with increasing temperature, accompanied by an increase in the corresponding acceptor ^{15}N7 chemical shifts. Above 35 °C, heterogeneity in the NMR spectra of the Na^+-bound DNA quadruplex indicated a melting of this species, whereas homogeneity is preserved up to 55 °C for the K^+- and NH_4^+-coordinated DNA quadruplexes. The largest relative decrease with temperature in $^{h2}J_{N2N7}$ couplings for the DNA quadruplexes, and thus the most thermolabile region, was identified to be the 5′ strand end constituting the G4*−G1, G1−G9*, and G10*−G2 H-bonds. The temperature dependence of $^{h2}J_{N2N7}$ couplings indicates a significantly higher thermal stability of the DNA quadruplexes compared to that of nucleic acid duplexes.

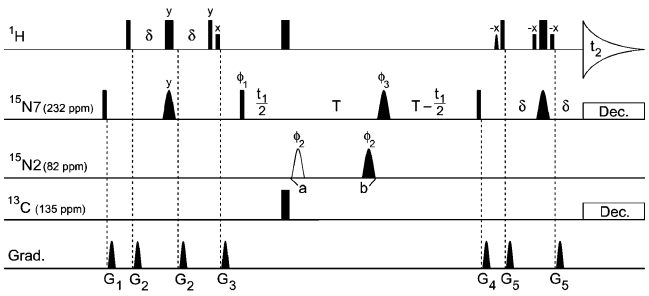

Figure 2. Pulse sequence of the quantitative J_{NN} constant-time spin−echo difference experiment. Narrow and wide pulses correspond to flip angles of 90 and 180°, respectively, and all pulse phases are *x* unless specified. Carrier positions are ^1H_2O (^{1}H) and 135 ppm (^{13}C). The ^{15}N carrier was placed in the center of the ^{15}N7 region (232 ppm) until point *a* in the sequence, when it was switched to the center of the ^{15}N2 region (82 ppm), and then switched back to 232 ppm at point *b*. All regular ^{1}H, ^{15}N, and ^{13}C pulses are applied at RF field strengths of 31, 1.25, and 16.7 kHz, respectively. Rectangular low-power ^{1}H pulses are applied using $\gamma_H B_1/2\pi$ = 200 Hz, and the sine-bell shaped $90°_{-x}$ pulse has a duration of 3.3 ms. The shaped ^{15}N7 180° pulses applied at the midpoint of each INEPT transfer period and during the 2*T* period have the shape of the center lobe of a (sin*x*)/*x* function with durations of 300 and 600 μs, respectively. The shaped ^{15}N2 180° pulse applied during 2*T* has a G3[46] amplitude profile, with a duration of 1.65 ms, corresponding to an inversion bandwidth of ±13 ppm. The positions of the filled and open ^{15}N2 inversion pulses correspond to the experiments where the $^{h2}J_{NN}$ coupling is active and inactive, respectively. WALTZ ($\gamma_N B_3/2\pi$ = 1.25 kHz) and GARP decoupling ($\gamma_C B_2/2\pi$ = 3.3 kHz) were applied during acquisition on the ^{15}N and ^{13}C channels, respectively. Delay durations: δ = 10 ms; *T* = 25 ms. Phase cycling: ϕ_1 = *x*, −*x*; ϕ_2 = 8(*x*), 8(−*x*); ϕ_3 = *x*, *x*, *y*, *y*, −*x*, −*x*, −*y*, −*y*; receiver = *x*, −*x*, −*x*, *x*. Quadrature detection in the t_1 period was achieved by incrementing ϕ_1 in the States-TPPI manner. Gradients are sine-bell shaped, with absolute amplitude of 25 G/cm at their center and durations (polarities) of $G_{1,2,3,4,5}$ = 2.8(−), 0.38(−), 3.0(+), 2.0(−), and 0.40(+) ms.

Results and Discussion

Experimental Approach used to Measure $^{h2}J_{NN}$ Couplings. The present study of Oxy-1.5 DNA covers a wide temperature range, and significant exchange broadening of amino donor resonances occurs at elevated temperatures. In this case, conventional donor−acceptor out-and-back experiments, such as the H2(N2)N7−COSY,[7,42] cannot be used for the quantitation of the $^{h2}J_{NN}$ couplings. An elegant approach to observe $^{h2}J_{NN}$ correlations despite the broadening of the donor resonances was proposed by Majumdar et al.,[43] where magnetization is excited on a nonexchanging proton H in the vicinity of the acceptor nitrogen N_a and is then transferred in an out-and-back manner by a direct coupling from H to N_a and then by $^{h2}J_{NN}$ to the donor N_d. Using a similar approach, all eight N2−H2···N7 H-bonds in the K^+-, Na^+-, or NH_4^+-loaded forms of Oxy-1.5 DNA could be observed as H8−(N7···N2) correlations with detection of the respective donor and acceptor ^{15}N frequencies (data not shown). However, due to the extended magnetization transfer delays, sensitivity and therefore precision of the derived $^{h2}J_{NN}$ values was limited.

A more sensitive approach consists of a simpler constant-time spin−echo (CTSE) difference method[44] that was previously used for the quantification of $^{h2}J_{NN}$ couplings in an A−A mismatch base pair.[45] The pulse scheme presented in Figure 2 is a modification of this experiment for the quantification of

(37) Sundquist, W. I.; Klug, A. *Nature* **1989**, *342*, 825−829.
(38) Phillips, K.; Dauter, Z.; Murchie, A. I.; Lilley, D. M.; Luisi, B. *J. Mol. Biol.* **1997**, *273*, 171−182.
(39) Hud, N. V.; Smith, F. W.; Anet, F. A.; Feigon, J. *Biochemistry* **1996**, *35*, 15383−15390.
(40) Deng, H.; Braunlin, W. H. *J. Mol. Biol.* **1996**, *255*, 476−483.
(41) Hud, N. V.; Schultze, P.; Sklenar, V.; Feigon, J. *J. Mol. Biol.* **1999**, *285*, 233−243.
(42) Dingley, A. J.; Masse, J. E.; Feigon, J.; Grzesiek, S. *J. Biomol. NMR* **2000**, *16*, 279−289.
(43) Majumdar, A.; Kettani, A.; Skripkin, E.; Patel, D. J. *J. Biomol. NMR* **2001**, *19*, 103−113.
(44) Grzesiek, S.; Vuister, G. W.; Bax, A. *J. Biomol. NMR* **1993**, *3*, 487−493.
(45) Majumdar, A.; Kettani, A.; Skripkin, E. *J. Biomol. NMR* **1999**, *14*, 67−70.

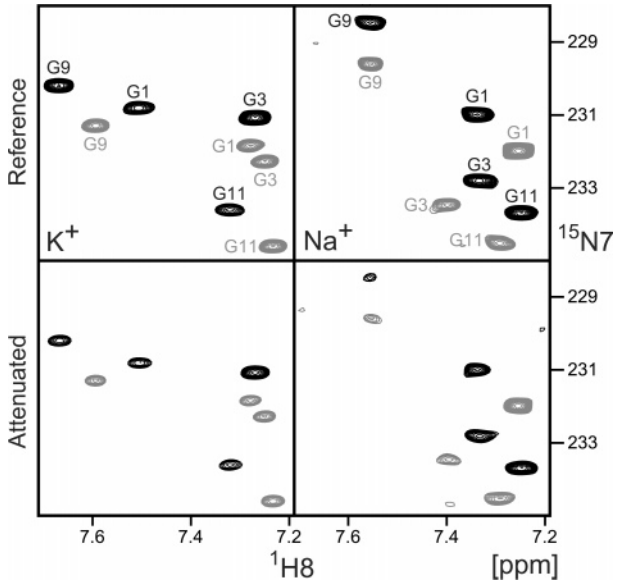

Figure 3. Overlay of a selected region of the CTSE difference experiment recorded at 5 (black contours) and 35 °C (gray contours) for the K^+ (left) and Na^+ (right) Oxy-1.5 DNA quadruplexes. The top row represents the reference experiment in which the $^{h2}J_{N2N7}$ coupling is inactive, whereas the bottom row shows the attenuated spectra due to the active $^{h2}J_{N2N7}$ coupling during the 2*T* period. Peaks are labeled with assignment information in the reference spectra.

$^{h2}J_{N7N2}$ couplings in the DNA quadruplex. Magnetization is transferred in an out-and-back manner from the ^{1}H8 to the ^{15}N7 nucleus whose chemical shift and $^{h2}J_{N7N2}$ coupling constant are determined in the constant time interval 2*T*. Selective sinc or G3[46] 180° pulses are used for excitation of the ^{15}N7 and ^{15}N2 nuclei in order to avoid undesirable loss of magnetization due to the presence of the relatively large one-, two-, and three-bond intranucleotide hetero- and homonuclear couplings.[47] In particular, the pulses avoid unwanted coupling between the ^{1}H8 proton and the ^{15}N9 nitrogen during the 2δ periods and provide selective transfer of magnetization across the H-bond between the ^{15}N7 and the ^{15}N2 during the 2*T* period. The size of the couplings is determined by recording a pair of ^{1}H−^{15}N CTSE spectra, with the $^{h2}J_{NN}$ coupling active or inactive during the constant time period 2*T*. This is achieved by altering the position of the selective inversion pulses on ^{15}N2 between positions a and b in Figure 2. As explained previously,[44] the value of $^{h2}J_{NN}$ is given by $\mathrm{acos}((I_{active}/I_{inactive}))/(2\pi T)$, where $I_{active}/I_{inactive}$ is the ratio of the cross-peak intensities derived from the two experiments.

Figure 3 shows the result of the CTSE difference experiment for the K^+ and Na^+ Oxy-1.5 quadruplexes recorded at 5 and 35 °C. Weaker peak intensities are clearly observed in the spectra recorded with the *trans*-H-bond couplings active between the donor N2 and acceptor N7 nuclei compared to the reference spectra, where the $^{h2}J_{NN}$ couplings are suppressed. This is particularly apparent for the resonance arising for the acceptor G9 N7 nucleus (G1−G9* H-bond) in the Na^+ Oxy-1.5 quadruplex, where the $^{h2}J_{N2N7}$ coupling (see below) is significantly stronger than all other $^{h2}J_{N2N7}$ couplings, in close agreement with the much shorter N−N distance observed in the crystal structure.

Comparison of the Different Ionic Forms of Oxy-1.5 DNA. Figure 4 shows a plot of the $^{h2}J_{N2N7}$ scalar couplings and the acceptor ^{15}N7 chemical shift of the K^+, Na^+, and NH_4^+ Oxy-1.5 DNA quadruplexes measured at 5, 15, 25, 35, 45, and 55 °C along with the N2···N7 distance (i.e., R_{N2}···N7) of the H-bonds from the Na^+-loaded[35] and K^+-loaded[36] Oxy-1.5 quadruplex X-ray and NMR structures. The eight $^{h2}J_{N2N7}$ scalar couplings correspond to a total of 16 N2−H2···N7 H-bonds since the two d($G_4T_4G_4$) monomers form a C_2-symmetric structure. The errors for the $^{h2}J_{NN}$ couplings are derived from the comparison of at least three datasets at each temperature and indicate a reproducibility that was, in most cases, better than 0.2 Hz, corresponding to a relative error in the coupling constants of maximally 3%. Only a few $^{h2}J_{N2N7}$ data points recorded for Na^+ Oxy-1.5 (in particular, G11−G10*) had larger errors, which correlate with significantly weaker peak intensities in the CTSE spectra. We attribute these intensity losses to chemical exchange broadening (data not shown). Such chemical exchange broadening is also observed in the G9*−G12 pair of the K^+-coordinated DNA quadruplex at 5 and 15 °C, where the $^{h2}J_{N2N7}$ correlations were below the detection limit in both the attenuated and reference CTSE $^{h2}J_{NN}$ spectra.

All the observed $^{h2}J_{N2N7}$ couplings of the different ionic forms of Oxy-1.5 (Figure 4) range between 6 and 8 Hz and are very similar to other $^{h2}J_{NN}$ couplings detected in various N−H···N H-bonds in duplex and triple-strand nucleic acids.[1,16] In many cases, the Na^+-bound form has the largest couplings, whereas K^+- and NH_4^+-bound forms have consecutively smaller couplings. It was important to determine whether such differences, which are on the order of 0.5 Hz, could be caused by direct electronic effects from the cations on the *trans*-H-bond couplings. Theoretical calculations carried out on the G-quartets bound to different monovalent cations indicate that such effects are negligible.[48] Thus, the observed differences in $^{h2}J_{N2N7}$ couplings between the different cation-bound forms of Oxy-1.5 DNA appear to reflect true structural and possibly dynamical differences in H-bond geometry. In particular, the larger size of $^{h2}J_{N2N7}$ in the Na^+-form indicates shorter N2···N7 H-bond distances. This correlates with the fact that the smaller Na^+ ion is located at the center of the G-quartet planes, whereas the larger K^+ and NH_4^+ ions reside between the planes (see Figure 1). Apparently, the Na^+ ion at the center of the G-quartets holds the N2−H2···N7 H-bonds of the guanosines more tightly together than the K^+ and NH_4^+ ions.

This is particularly evident for the base pairs G1−G9* and G11−G10*, where $^{h2}J_{N2N7}$ values are larger by 0.5−1 Hz for the Na^+-bound form as compared to the values of the K^+/NH_4^+-bound forms. Examination of the DNA quadruplex structure shows that these two H-bonds are located in one corner of Oxy-1.5 (Figure 1A). The smaller $^{h2}J_{N2N7}$ value for the G1−G9* H-bond of the K^+-bound form is in agreement with a significantly longer $R_{N2\cdots N7}$ observed in the crystal structure (2.78 ± 0.08 Å) versus the Na^+-bound form (2.62 ± 0.03 Å) (Figure 4). Angular variations between both forms are expected to play only a minor role since the H-bonds are rather straight and the various H-bond angles in both structures have rather similar values (data not shown). The larger G1−G9* $^{h2}J_{N2N7}$ coupling

(46) Emsley, L.; Bodenhausen, G. *Chem. Phys. Lett.* **1990**, *165*, 469−476.
(47) Ippel, J. H.; Wijmenga, S. S.; de Jong, R.; Heus, H. A.; Hilbers, C. W.; de Vroom, E.; van der Marel, G. A.; van Boom, V. A. *Magn. Reson. Chem.* **1996**, *34*, S156−S176.
(48) van Mourik, T.; Dingley, A. J. *Chem.−Eur. J.* **2005**, in press.

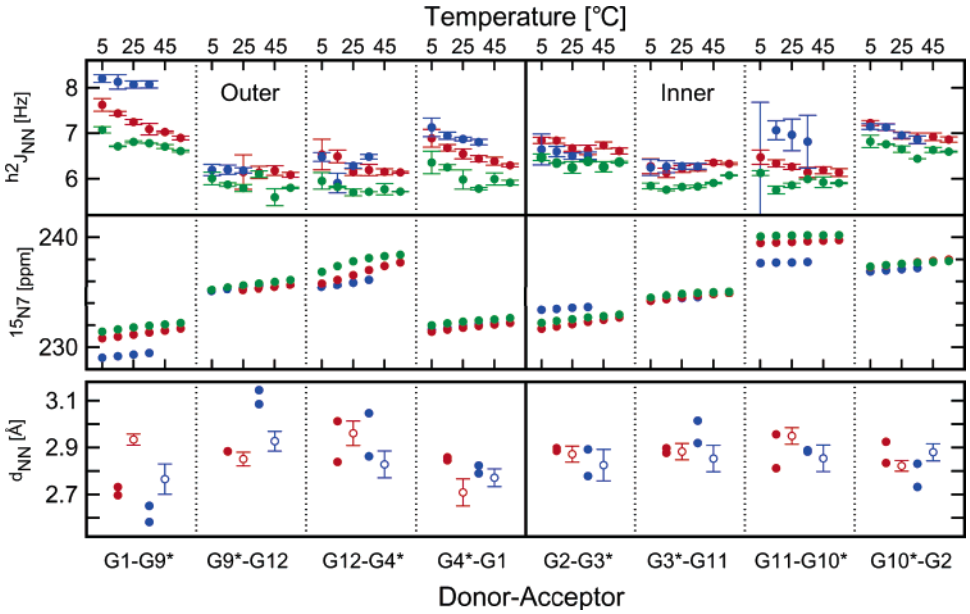

Figure 4. H-bond parameters of the Na^+ (blue), K^+ (red), and NH_4^+ (green) Oxy-1.5 DNA quadruplexes. Top rows: temperature dependence of $^{h2}J_{NN}$ couplings and acceptor $^{15}N7$ chemical shifts. For each H-bond, data are depicted in equidistant spacing from left to right for the six temperatures of 5, 15, 25, 35, 45, and 55 °C. The $^{h2}J_{NN}$ correlation for the G11−G10* H-bond in the Na^+-coordinated DNA quadruplex at 5 °C was only observable in the reference CTSE spectra. As previously described,[16] an upper limit for this $^{h2}J_{NN}$ coupling was derived from the ratio of the lowest plotted contour level in the attenuated spectrum relative to the peak height in the reference spectrum. Bottom row: H-bond N2···N7 lengths derived from the Na^+ and K^+ Oxy-1.5 DNA quadruplex crystal structures (closed circles) and the average (with standard deviations) of the 10 lowest energy NMR structures (open circles) for the outer and inner G-quartets.

constants in the Na^+-bound form coincide with smaller values of the acceptor G9* $^{15}N7$ chemical shift values as compared to the other ionic forms. DFT calculations[18] have shown previously that both smaller acceptor ^{15}N shifts and larger $^{h2}J_{NN}$ couplings are expected for shorter H-bonds because the decrease of the N−N length leads to increased hydrogen/acceptor orbital overlap and increased shielding of the acceptor nucleus. A similar increase of the $^{h2}J_{N2N7}$ coupling and decrease of the $^{15}N7$ chemical shift is observed for the G11−G10* base pair in the Na^+-bound form. However, this NMR evidence for a shorter H-bond does not correspond to a clear trend for the $R_{N2\cdots N7}$ distances in the crystal or solution structures[35] (Figure 4). Thus, this new $^{h2}J_{N2N7}$ coupling and $^{15}N7$ shift evidence may indicate a genuine structural difference between the Na^+- and K^+-bound forms in solution, which was not picked up in the previous NMR structure determinations due to the limited precision of NOE-derived distances. The particularly strong H-bond coupling for the G11−G10* N2−H2···N7 H-bond also coincides with the fact that the G11 amino protons are the most slowly exchanging ($k_{ex} \sim 1$ week^{-1}) of all the amino groups in the Na^+-bound form.[49]

A further genuine difference between solution and crystal forms appears for the G9*−G12 base pair: the $R_{N2\cdots N7}$ distance in the crystal structure of the Na^+-bound DNA quadruplex is considerably longer (~0.2 Å) than in the K^+-coordinated form (and also longer than for all other N−H···H bonds of both crystalline forms). Such an H-bond lengthening should correspond to a decrease of about 2 Hz in the $^{h2}J_{NN}$ coupling.[18] Yet, the observed $^{h2}J_{N2N7}$ couplings are very similar (~0.1 Hz) in magnitude (Figure 4). In contrast to the crystal structure, the average $R_{N2\cdots N7}$ distance derived from the NMR structures of the Na^+ DNA quadruplex is similar in value to the $R_{N2\cdots N7}$ distance in the K^+ DNA quadruplex structure. Thus, it is likely that crystal packing effects and/or the co-crystallization of the Na^+ DNA quadruplex with the telomere end-binding protein[35] have caused a deformation of the G9*−G12 base pair that is not present in the solution structure. This conclusion is supported by recent density functional theory calculations of $^{h2}J_{N2N7}$ couplings, which severely underestimate the $^{h2}J_{N2N7}$ coupling for the G9*−G12 base pair when using the geometric coordinates of the G-quartets derived from the Na^+ DNA quadruplex crystal structure.[48]

No crystal structure is available for the NH_4^+-bound form of Oxy-1.5. However, NMR studies suggest that the coordination of the NH_4^+ cations in the Oxy-1.5 quadruplex is similar to that observed for the K^+-bound Oxy-1.5 quadruplex structure.[34,41] The majority of the $^{h2}J_{N2N7}$ couplings in the NH_4^+ form are weaker than those in the Na^+- and K^+-coordinated DNA quadruplexes. This could result from expansion of the base pairs due to the G-quartets opening to accommodate the coordination and movement of the slightly larger ionic radius of 1.43 Å for the NH_4^+ ion compared to the ionic radius of 1.33 Å for the K^+ ion. In addition to potential geometric factors influencing the size of the $^{h2}J_{NN}$ values, the impact of the coordinated NH_4^+ ion to the electron density associated with the N2−H2···N7 H-bond moieties may also influence the size of the electron-mediated $^{h2}J_{NN}$ scalar couplings. Previous results[41] indicate that the NH_4^+ moves significantly more slowly through the DNA quadruplex than K^+,[41] and this may be due to H-bonding between the guanosine carbonyl groups and the ammonium protons. Such H-bonding could cause a weakening of the electron density associated with the N2−H2···N7 H-bonds and reduce the magnitude of the $^{h2}J_{NN}$ values. However, theoretical calculations at the HF/6-31G(d) level of theory using a C_{4h}-symmetric G-quartet model show that the presence of the

(49) Smith, F. W.; Feigon, J. *Biochemistry* **1993**, *32*, 8682−8692.

NH_4^+ ion has no significant influence on the size of the $^{h2}J_{NN}$ couplings (data not shown) and causes only small decreases in the absolute size of the $^{h3}J_{NC'}$ and $^{1}J_{N1H1}$ couplings, presumably due to a decrease of electron density in the N1−H1···O6═C6 and N1−H1 moieties. Consequently, the observation of weaker $^{h2}J_{NN}$ couplings cannot be attributed to a direct electronic effect by the NH_4^+ ions and is most likely caused by an expansion of the DNA quadruplex to allow movement of the NH_4^+ ions through the central cavity.

Temperature Dependence. A. General Behavior of Na^+-, K^+-, NH_4^+-Bound Forms. Above 35 °C, significant heterogeneity was observed in the quantitative J_{NN} CTSE spectra recorded on the Na^+ Oxy-1.5 DNA quadruplex, thus making the quantitative analysis of the $^{h2}J_{N2N7}$ couplings at 45 and 55 °C very difficult (data not shown). The analysis was therefore restricted to the range between 5 and 35 °C. The spectral heterogeneity above 35 °C indicates that the Na^+ Oxy-1.5 DNA quadruplex melts between 35 and 45 °C. This finding agrees with circular dichroism studies on the Na^+-bound form of *Oxytricha nova* DNA quadruplex (i.e., $d(T_4G_4)$) in which a melting temperature of ∼40 °C was found.[50] In contrast to the Na^+-bound quadruplex, spectral homogeneity for the K^+- and NH_4^+-coordinated quadruplexes persists up to 55 °C. This is in agreement with previous thermal denaturation studies that indicate a higher thermal stability for the K^+-bound quadruplex as compared to that for the Na^+-bound form.[50] It is interesting that the Na^+-bound quadruplex melts at the lowest temperature even though the *J* couplings indicate that it has, in general, the shortest N2−H2···N7 H-bond distances. This would seem to indicate that the overall stability is determined by the cation coordination, rather than H-bond length or strength. These results are consistent with a previous thermodynamic analysis that indicated that although Na^+ has a more favorable intrinsic free energy of binding, the K^+-bound quadruplexes are more thermally stable due to the greater energetic cost of Na^+ dehydration versus K^+.[39]

B. Temperature Dependence of $^{h2}J_{N2N7}$. It is evident from the temperature dependence in Figure 4 that the size of the $^{h2}J_{N2N7}$ couplings decreases with increasing temperature for all H-bonds. This corresponds to an average weakening of donor−acceptor overlap at higher temperatures. Similar to the correlation observed for the different types of bound cations, the decrease in $^{h2}J_{N2N7}$ coincides with an increase of the acceptor ^{15}N7 chemical shift resulting from the decrease in shielding for longer H-bonds.[18] Within experimental error, the decrease in $^{h2}J_{N2N7}$ appears approximately linear. Differences are apparent in the slopes of the $^{h2}J_{N2N7}$ couplings for individual H-bonds.

Figure 5 shows these slopes in the form of an average relative decrease with temperature, $\Delta^{h2}J_{N2N7}/\Delta T/\langle^{h2}J_{N2N7}\rangle$, where $\Delta^{h2}J_{N2N7}/\Delta T$ was obtained from a linear fit to the data in Figure 4, and $\langle^{h2}J_{N2N7}\rangle$ represents the individual mean value. The expression $\Delta^{h2}J_{N2N7}/\Delta T/\langle^{h2}J_{N2N7}\rangle$ derives its justification from the approximately exponential distance dependence of H-bond *J* couplings, that is, $^{h2}J_{NN} \approx A \times \exp(-k_R \times r_{NN})$, where k_R represents an exponential decay constant, which is approximately 2.3 $Å^{-1}$, as derived by DFT calculations for Watson−Crick and Hoogsteen base pairs.[18] A similar k_R value of 2.0 $Å^{-1}$ has recently been derived by DFT calculations on Hoogsteen G−G base pairs in G-quartets.[48] Thus, $\Delta^{h2}J_{N2N7}/\Delta T/\langle^{h2}J_{N2N7}\rangle \approx \mathrm{d}\ln{}^{h2}J_{N2N7}/\mathrm{d}T = -k_R \times \mathrm{d}r_{NN}/\mathrm{d}T$ represents an approximate measure of the linear expansion of the H-bond that can be translated into a linear thermal expansion coefficient, $\alpha_L = 1/r_{NN} \times \mathrm{d}r_{NN}/\mathrm{d}T \approx 1/(-k_R \times r_{NN}) \times (\Delta^{h2}J_{N2N7}/\Delta T/\langle^{h2}J_{N2N7}\rangle)$.[21]

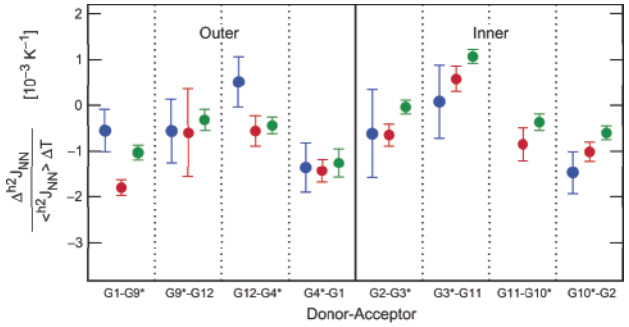

Figure 5. $\Delta^{h2}J_{N2N7}/\Delta T/\langle^{h2}J_{N2N7}\rangle$ values for each N2−H2···N7 H-bond in the Na^+ (blue), K^+ (red), and NH4$^+$ (green) Oxy-1.5 DNA quadruplexes. $\Delta^{h2}J_{N2N7}/\Delta T$ values were derived from a linear fit to the data in Figure 4, and $\langle^{h2}J_{N2N7}\rangle$ represents the individual mean values. Errors for $\Delta^{h2}J_{N2N7}/\Delta T/\langle^{h2}J_{N2N7}\rangle$ were obtained by error propagation.

Clearly, the errors for $\Delta^{h2}J_{N2N7}/\Delta T/\langle^{h2}J_{N2N7}\rangle$, as derived by error propagation (Figure 5), are considerable. However, certain trends are apparent. The relative changes in $\Delta^{h2}J_{N2N7}/\Delta T/\langle^{h2}J_{N2N7}\rangle$ for most H-bonds are smaller in absolute size than 1×10^{-3}/K. Notable exceptions are the N2−H2···N7 H-bonds of base pair G4*−G1 (and symmetry-related G1−G4*) for all cation-bound forms ($\Delta^{h2}J_{N2N7}/\Delta T/\langle^{h2}J_{N2N7}\rangle \approx -1.4 \times 10^{-3}$/K) and base pair G1−G9* (G1*−G9) for the K^+-bound form (-1.8×10^{-3}/K). Therefore, these H-bonds in the quartets appear as the most thermolabile in the molecule. A rationale for the behavior of the G4*−G1 H-bond may be its location at the 5′ strand end, which is apparently affected by fraying. In accordance with this finding, the N2−H2···N7 H-bond of G10*−G2, that is, the H-bond closest to the 5′ strand end in the inner quartet, has the strongest relative decrease $\Delta^{h2}J_{N2N7}/\Delta T/\langle^{h2}J_{N2N7}\rangle$ within the inner quartet (Figures 4 and 5). The strong decrease of $^{h2}J_{N2N7}$ for G1−G9* of the K^+-bound form is remarkable since the Na^+- and NH_4^+-bound forms show a significantly lower decrease (Figures 4 and 5). Apparently, the binding of potassium between the G-quartets and within the T_4-loop (Figure 1) destabilizes the N2−H2···N7 H-bond between G1 and G9*.

A further general observation may be made from the absolute size of $\Delta^{h2}J_{N2N7}/\Delta T/\langle^{h2}J_{N2N7}\rangle$ in the G-quadruplexes. The temperature dependence of $^{h2}J_{NN}$ couplings has been investigated before for Watson−Crick base pairs in short DNA duplexes[20] and a 22-nucleotide RNA hairpin.[23] For base pairs in regular stem regions, the limited data of both studies are very similar for Watson−Crick A·U, A·T, and G·C base pairs and show a relative decrease $\Delta^{h2}J_{NN}/\Delta T/\langle^{h2}J_{NN}\rangle$ of about $-(2-3) \times 10^{-3}$/K, whereas a stronger decrease occurs for a Watson−Crick U·A base pair next to a noncanonical G·U pair ($\approx -6 \times 10^{-3}$/K).[23] In the three cation-bound forms of the DNA quadruplexes, the relative decreases $\Delta^{h2}J_{N2N7}/\Delta T/\langle^{h2}J_{N2N7}\rangle$ for all N2−H2···N7 H-bonds are significantly smaller than the reported values for the nucleic acid duplexes (Figure 5), with the sole exception of the fraying G1−G9* base pair in the K^+-bound form. Therefore, the temperature dependence of $^{h2}J_{N2N7}$ indicates a significantly higher stability of the N−H···N H-bonds in the DNA quadruplex as compared to that in the nucleic acid

(50) Lu, M.; Guo, Q.; Kallenbach, N. R. *Biochemistry* **1992**, *31*, 2455−2459.

duplexes. This robustness to thermal expansion is not surprising when one considers the constraints that are exerted onto the DNA quadruplex structure by the cation coordination, the extensive H-bond networks, steric restriction within the G-quartets, and the stacking interactions.

Conclusion

A comparison of the $^{h2}J_{N2N7}$ couplings describing the N2−H2···N7 H-bond properties as a function of temperature has been presented for the Na^+, K^+, and NH_4^+ forms of the Oxy-1.5 quadruplex. The variations in $^{h2}J_{N2N7}$ couplings between DNA quadruplex species reflect structural differences in H-bond geometries. The overall larger magnitude of the $^{h2}J_{N2N7}$ couplings for the Na^+ form is attributed to the different coordination of the Na^+ ions as compared to that of the K^+/NH_4^+ ions. The Na^+ ion, which is located in the center of the G-quartet planes, holds the N2−H2···N7 H-bonds more tightly together than the K^+ or NH_4^+ ions, which are positioned between the G-quartets. The temperature dependence of the $^{h2}J_{N2N7}$ couplings indicates a general expansion of the H-bonds at higher temperatures. For the Na^+-coordinated DNA quadruplex, spectral heterogeneity above 35 °C indicates a partial melting of the structure, whereas the K^+/NH_4^+-bound structures remain intact up to 55 °C. The analysis of individual H-bond $^{h2}J_{N2N7}$ couplings reveals that N2−H2···N7 H-bonds at the 5′ strand end are the least thermostable in all three cationic forms of the quadruplex. This reveals a likely unfolding pathway common to all cationic forms of this quadruplex. The decrease of all $^{h2}J_{N2N7}$ couplings with increasing temperature is significantly smaller than comparable values in nucleic acid duplexes. The cation coordination of the G-quartets and the extensive H-bond networks of the G-quadruplex structures rationalize this particular thermal stability.

Material and Methods

The uniformly ^{13}C,^{15}N-labeled d($G_4T_4G_4$) quadruplex was synthesized as previously described.[51] NMR experiments were carried out on a Shigemi microcell sample of 270 μL volume containing 1.1 mM DNA quadruplex (2.2 mM oligomer) in either 50 mM NaCl, KCl, or NH_4Cl and 95% H_2O/5% D_2O at pH 6.55. To exchange the type of monovalent ion present in the sample, the DNA sample was desalted on a G25 column and passed over a Bio-Rad AG-50 cation exchange column that had been charged with the chosen monovalent ion. All NMR spectra were recorded on Bruker DRX-500 or DRX-600 NMR spectrometers equipped with standard 5 mm triple-axis pulsed field gradient $^1H/^{15}N/^{13}C$ probehead optimized for ^1H detection. NMR data sets were processed using the program nmrPipe,[52] and peak positions and integrals were determined with the program PIPP.[53] For determining the hydrogen bond distances and angles, hydrogen atoms were added to the sodium (PDB entry 1JB7) and potassium (PDB entry 1JPQ) Oxy-1.5 crystal structures with the program XPLOR,[54] using ideal covalent geometry and a guanosine N2−H2 and N1−H1 distance of 1.03 Å. The same value was used for the thymine N3−H3 distance.

$^{h2}J_{NN}$ *trans*-H-Bond Scalar Couplings. The selective pulse quantitative J_{NN} constant-time spin−echo (CTSE) difference experiment depicted in Figure 1 was used to measure the $^{h2}J_{NN}$ *trans*-H-bond scalar coupling constants. The quantitative J_{NN} CTSE spectra were recorded at six temperatures (5, 15, 25, 35, 45, 55 °C) as data matrices of 54* (t_1) × 512* (t_2) data points (where n* refers to the number of complex points) with acquisition times of 49 ms (t_1) and 55 ms (t_2). Depending on temperature, total measuring time ranged from 1 to 8 h for a single spectrum. To judge the experimental reproducibility, both inactive (reference) and active coupling experiments were carried out at least three times at every temperature, and the reported values for $^{h2}J_{NN}$ couplings and their errors refer to mean and standard deviations derived from these independent measurements. Proton chemical shifts were referenced relative to 3,3,3-trimethylsilyl propionic acid (TSP). ^{15}N chemical shifts were referenced indirectly relative to the TSP ^1H frequency.[55]

Acknowledgment. A.J.D. thanks Dr. Mark Williams for providing software to calculate various geometric parameters. This work was funded by NIH Grant GM48123 to J.F. and SNF Grant 31 43'091.95 to S.G.

JA0540369

(51) Masse, J. E.; Bortmann, P.; Dieckmann, T.; Feigon, J. *Nucleic Acids Res.* **1998**, *26*, 2618−2624.
(52) Delaglio, F.; Grzesiek, S.; Vuister, G. W.; Zhu, G.; Pfeifer, J.; Bax, A. *J. Biomol. NMR* **1995**, *6*, 277−293.
(53) Garrett, D. S.; Powers, R.; Gronenborn, A. M.; Clore, G. M. *J. Magn. Reson.* **1991**, *95* 214−220.
(54) Brünger, A. *XPLOR*. Yale University, New Haven, CT, 1992.
(55) Markley, J. L.; Bax, A.; Arata, Y.; Hilbers, C. W.; Kaptein, R.; Sykes, B. D.; Wright, P. E.; Wuthrich, K. *J. Biomol. NMR* **1998**, *12*, 1−23.